Journal of Drug Delivery Science and Technology 84 (2023) 104469

Contents lists available at ScienceDirect

Journal of Drug Delivery Science and Technology

journal homepage: www.elsevier.com/locate/jddst

3D printing fabrication of Ethylene-Vinyl Acetate (EVA) based intravaginal rings for antifungal therapy

Sofia Moroni, Francesca Bischi, Annalisa Aluigi, Raffaella Campana, Mattia Tiboni *, Luca Casettari

Department of Biomolecular Sciences, University of Urbino Carlo Bo, Piazza del Rinascimento, 6, 61029, Urbino, PU, Italy

ARTICLE INFO

Keywords:
Additive manufacturing
Fused deposition modeling
Hot-melt extrusion
Personalized medicine

ABSTRACT

Vulvovaginal candidiasis is a vaginal infection that affects women of reproductive age. Nowadays, the high administration frequency of conventional antifungal formulations, and recurrences negatively impact patients' well-being. In this context, intravaginal rings (IVRs) offer the possibility of controlled local drug delivery with one single application, thus possibly increasing patient compliance. This project aimed to fabricate 3D printed IVRs to highlight the potential application of these medical devices for antifungal therapy, as well as emphasize the employment of 3DP as alternative manufacturing tool. Ethylene-Vinyl Acetate copolymer was chosen as matrix, and the antifungal efficacy of bifonazole and clotrimazole loaded in the IVRs was compared. The resulting medical devices were characterized using Fourier Transformed Infrared spectroscopy, the thermal behavior was investigated with Thermogravimetric Analysis and Differential Scanning Calorimetry, proving the stability of the incorporated drugs. In addition, the drug release profile was evaluated in a vaginal fluid simulant pH 4.2, at 37 °C, showing a sustained release over a week. The compressive strength of the IVRs was investigated, confirming that the mechanical properties comply with the already commercialized devices. To evaluate the antifungal activity, an *in vitro* time-kill assay was performed against *Candida albicans* for 7 days, exhibiting a complete growth inhibition after 4 days for the 3D printed IVRs. Overall, this work represents a step forward in the production of 3D printed IVRs potentially able to exert antifungal activity with one single application.

1. Introduction

Vulvovaginal candidiasis (VVC) is a frequent and common infection of the vulva and/or vagina predominantly caused by the pathogen fungus *Candida albicans*, or related fungi. After bacterial vaginosis, it is the second most common cause of vaginal infections, affecting millions of women every year [1]. *C. albicans* is commonly found on the mucous surfaces of the human body, being part of the quiescent flora. However, changes in the environment can promote proliferation and infection development, characterized by the following symptoms including itching, vaginal soreness, irritation, burning, swelling, dyspareunia, external dysuria, and abnormal vaginal discharge [2,3]. The pathogenesis depends on the virulence of the *Candida* and on the defence mechanisms of the individual. Some predisposing factors and triggering mechanisms have been identified, such as the use of antibiotics, uncontrolled diabetes, use of contraceptives, and hormonal genetic and lifestyle-related factors [4–6].

The conventional treatment of candidiasis consists in administering antifungal drugs, available in a variety of standard formulations, such as pessaries or creams, for a duration from three to seven days [7]. Among antifungal drugs, the class of imidazoles is still considered the first-line treatment for *C. albicans* infections. This class of drugs inhibits the enzyme lanosterol 14-alpha-demethylase, cytochrome P450 dependent, which is essential for sterols biosynthesis. Moreover, given the high incidence of recurrences, the maintenance regimen is recommended including oral weekly antifungal drugs for up to 6 months [8]. Despite the therapeutic advances, the high frequency of treatment administration, the onset of symptoms, microbial resistance, and recurrences still impact the psychological well-being of patients, resulting in poor compliance [9,10]. Thus, finding an efficient strategy is needed. Recently, topical solid vaginal formulations have aroused great interest, including IVRs [11]. IVRs are flexible medical devices that provide a continuous and sustained, or controlled local delivery of the drug incorporated, with a single application [12]. Commonly, they are

* Corresponding author.
E-mail address: mattia.tiboni@uniurb.it (M. Tiboni).

https://doi.org/10.1016/j.jddst.2023.104469
Received 13 January 2023; Received in revised form 7 April 2023; Accepted 13 April 2023
Available online 15 April 2023
1773-2247/© 2023 The Authors. Published by Elsevier B.V. This is an open access article under the CC BY license (http://creativecommons.org/licenses/by/4.0/).

manufactured by hot melt extrusion (HME) or injection moulding (IM), using silicone elastomer and polyurethane [13]. Based on the advantages conferred, such as the safety and the low side effects, IVRs are well-accepted by women [14] being already established for hormonal therapy [15]. Additionally, their feasibility and efficacy in other applications associated with women's health have been investigated (*e.g.*, for the overactive bladder treatment [16], for the prevention of sexually transmitted diseases [17], and as cervical ripening agents [18]). However, at present, their application for antifungal treatment has been poorly explored.

Our group has previously demonstrated the possibility to produce antifungal IVRs by 3D printing using thermoplastic polyurethane [19].

The employment of 3DP rather than IM, as manufacturing tool, enables the production of cost-effective small batches, centred on the patient's need or useful for clinical studies. Complex geometries can be produced, and the size and doses can be easily customized thanks to 3DP that allows rapid prototyping [20,21]. Recently, few applications of 3DP in the production of intravaginal devices have been reported [22–24].

This project aimed to make a step forward on the development of a new generation of 3D printed IVRs, for the treatment of recurrent fungal infections. For this purpose, ethylene-Vinyl Acetate (EVA) copolymer was chosen as matrix and the loading and efficacy of bifonazole (BFZ) and clotrimazole (CTZ) as antifungal imidazole drugs was compared.

EVA is a biocompatible, insoluble, and non-toxic thermoplastic copolymer of ethylene and vinyl acetate, which has FDA approval, and it is a plastic material suitable to produce particularly elastic products, which stand out for their softness and flexibility [25,26]. In recent years, thermoplastic EVA copolymers have shown great potential for the manufacturing of sustained-release matrices. An example of an EVA-based device, that is available on the market, is the contraceptive IVR Nuvaring®, where the active pharmaceutical ingredients (API) (etonogestrel and ethinylestradiol) are homogeneously distributed within the core polymer [27].

Herein, IVRs were 3D printed with Fused Deposition Modeling (FDM) technique, coupled with HME to produce the filaments needed for the printing process. FDM is commonly use in the pharmaceutical field, being versatile, low cost and given the wide range of material available [28]. After an initial characterization comprising size, weight, and drug content homogeneity, the chemical composition, thermal studies and mechanical properties were evaluated. Furthermore, the release profile was investigated using a mixture of water/ethanol, for quality control intent and a vaginal fluid simulant (VFS) at pH 4.2 to better mimic the *in vivo* environment. Finally, to assess the antifungal potentiality of the devices, the *in vitro* antifungal activity was investigated against *C albicans* for up to 7 days.

2. Materials and methods

2.1. Materials

EVA1070 copolymer (EVA, Ateva®), in micronized powder form was kindly donated by Celanese Corporation (Germany – USA). The key characteristics of the polymer are a VA content of 9%, tensile strength at break of 17–18 MPa, elongation at break of 400–600%, and flexural modulus of 101 MPa. Bifonazole (BFZ) was purchased from BLD pharm (Germany); while clotrimazole (CTZ) was purchased from Tokyo Chemical Industry (Japan). Methanol, Ethanol, Acetonitrile (ACN), Trifluoracetic acid (TFA), sodium chloride, glacial acetic acid, and formic acid were purchased from Merck (Germany). Lactic acid was purchased from A.C.E.F. (Italy). All solvents used were HPLC grade.

2.2. Methods

2.2.1. Preparation of EVA filaments containing BFZ and CTZ by HME

For the fabrication of 3D printed IVRs, FDM feeding filaments were prepared using HME. For this purpose, EVA in micronized form was mixed with 10% w/w of BFZ or 10% w/w of CTZ. Mixture homogeneity was ensured using a mechanical mixer (Galena Top powder mixer, Ataena, Italy) at a constant speed for 30 min. The resulting blends were fed in the filament extruder (Noztek Pro HT, 3 mm nozzle, Noztek, UK), equipped with a stainless-steel barrel and screw, and extruded at 170 °C for BFZ and 155 °C for CTZ. Blank filaments were produced by feeding the extruder with pure EVA and extruded at a temperature of 150 °C (Table 1). The final filaments' diameters ranged between 2.75 and 2.85 mm.

2.2.2. Fabrication of 3D printed IVRs containing BFZ and CTZ by FDM 3D printing

Drug-loaded and blank IVRs were printed with the prepared filaments using an Ultimaker 3 FDM 3D printer (Ultimaker, The Netherlands). The ring model was designed with a CAD-based software and then converted to a print pattern using Ultimaker Cura 5.0 software (Ultimaker, The Netherlands). The printing parameters were set as follows: layer height 0.1 mm with 100% of infill density and printing speed of 25 mm/s. The printing temperatures, reported in Table 1, were 190 °C both for the blank and CTZ-loaded rings, and 200 °C for the ring containing BFZ. The build plate was always kept at 60 °C.

2.2.3. Characterization of 3D printed IVRs

After printing, the IVRs were weighed and the outer diameter (OD) and the cross-sectional diameter (CSD) were measured using a digital calliper (Mitutoyo, Japan), taking care to ensure that the IVRs were not compressed or distorted during measurements. In addition, filaments and the printed rings were observed with a stereo microscope (Nikon SMZ-1, Nikon, Japan).

2.2.3.1. Homogeneous distribution of the drug. To evaluate the homogeneous distribution of the drugs in the device, different samples were cut from the printed rings and placed in ethanol for 48 h under gentle stirring. The amount of BFZ and CTZ released was measured by High Performance Liquid Chromatography (HPLC, Agilent 1260 Infinity II, Agilent, USA). The analysis was conducted with a flow rate of 1 mL/min in an Agilent Zorbax Eclipse Plus C18, 150 × 4.6 mm, 5 μm column (Agilent, USA), keeping the analysis system at room temperature. For BFZ, 0.05% TFA in water and 0.1% TFA in methanol (ratio 30:70) were selected as mobile phases; the injection volume was 10 μL and the detection signal was recorded at 250 nm. While for CTZ, a mixture of 0.5% FA in water and acetonitrile (ratio 55:45) were selected as mobile phases and the detection signal was recorded at 230 nm.

Furthermore, the homogeneous distribution of the drug among the IVRs was confirmed using Fourier-transform infrared spectroscopy (FTIR, Spectrum Two FT-IR spectrometer with ATR accessory, PerkinElmer, MA, USA), by comparing the chemical composition of the printed devices with the starting materials. For this purpose, measurements were performed at 450-4000 cm^{-1} with a resolution of 4 $cm^{-1}$and a total of 64 scans.

2.2.3.2. Thermal behaviour. The thermal behaviour of the raw materials and the printed devices was assessed using Thermogravimetric Analysis (TGA) and Differential Scanning Calorimetry (DSC). For TGA, (TGA PerkinElmer 4000, PerkinElmer, MA, USA) scans were run from room temperature to 500 °C, at a speed rate of 10 °C/min under a nitrogen flow rate of 30 mL/min.

Table 1
Optimization of HME and FDM parameters used during the production of the IVRs.

Material	Extrusion Temperature (HME)	Printing Temperature (FDM)
EVA	150 °C	190 °C
EVA + 10% BFZ	170 °C	200 °C
EVA + 10% CTZ	155 °C	190 °C

For DSC (DSC PerkinElmer 6000, PerkinElmer, MA, USA), approximately 3 mg of each sample were placed in aluminium pans and were heated up with a fixed heating rate of 10 °C/min from 30 to 200 °C, cooled down at a fixed cooling rate of 5 °C/min to −30 °C and heated up again to 200 °C. Samples were analyzed directly after the preparation and after storage for 4 weeks under ambient condition, away from light. All thermal data were analyzed by Pyris Manager software (PerkinElmer, MA, USA). The crystallinity degree (χ) was calculated according to equation (1).

$$\chi(\%) = [\Delta H_m/(\Delta H_m^*)]*100 \quad (1)$$

Where the ΔH_m and $\Delta H_m^*$are the melting enthalpies of the analyzed sample and the enthalpy of the 100% crystalline polyethylene ($\Delta H_m^* = 287.3\ J\ g^{-1}$) respectively.

2.2.4. In vitro BFZ and CTZ release study

For the release study, the 3D printed IVRs were placed in sealed glass bottles with 100 mL of release medium (50% Ethanol in water) or VFS [29]. The VFS was composed as follow: bovine serum albumin (18 mg/L), NaCl (3.5 g/L), KOH (1.4 g/L), $Ca(OH)_2$ (0.22 g/L), lactic acid 90% (2.2 g/L), glycerol 50% (0.32 g/L), urea (0.4 g/L), glacial acid acetic (1 g/L), glucose (0.5% w/v) adjusted to pH 4.2. The bottles were kept at 37 °C under gentle stirring (100 rpm) for seven days. 1 mL of each sample was withdrawn every 2 h for the first 6 h, then every 24 h, replacing the volume with fresh medium, preheated at the same temperature. The amount of BFZ and CTZ released from the IVRs was measured with HPLC as reported above (section 2.2.3.1). Experiments were conducted in triplicate.

2.2.5. Mechanical properties

The compressive behaviour of the IVRs was evaluated using a TA texture analyser (TA.XT plus Texture Analyzer, Stable Micro Systems, UK), fitted with a 50 Kg load cell. IVRs were placed vertically and compressed of 5 mm at a 2 mm/s speed. To keep the IVRs in the vertical position, a custom-made holder was 3D printed and assembled to the platform of the instrument. The maximum forces required to compress the IVRs were recorded. Six measurements were performed for each IVR, testing different areas of the device.

2.2.6. Microbial strain and culture conditions

In this study, the reference strains *Candida albicans* ATCC 10231 was selected. The strain was grown on Sabouraud Dextrose Agar (SDA) plates (VWR, Milan, Italy) at 37 °C for 24 h, while the stock cultures were kept at −80 °C in Nutrient Broth (VWR) with 15% of glycerol.

2.2.7. Minimum inhibitory concentration (MIC) determination of both BFZ and CTZ

The MIC of each drug was determined following the standard microdilution method [30]. As first, BFZ and CTZ stock solutions were prepared in DMSO of biological grade (2 mg/mL) and stored at 4 °C in the dark. *C. albicans* ATCC 10231 was incubated in Tryptone Soy Broth (TSB, VWR) (20 mL) for 24 h at 37 °C. Afterwards, the microbial suspension was spectrophotometrically adjusted ($OD_{600\ nm}$) to 0.13–0.15 corresponding to about 10^6 CFU/mL. Then, 100 μL of this suspension was diluted 1:50 in standard RPMI 1640 medium (Sigma-Aldrich, Milan, Italy) and inoculated into a 96-well plate together with the adequate volumes of BFZ and CTZ solution (0.0625–16 μg/mL). Two rows inoculated with medium without the antifungal agent (control growth) and one with only medium (negative control) were considered. Preliminary tests were performed with DMSO to exclude its possible antifungal activity; in any case, the volume of DMSO never exceeded 5% (v/v). All the plates were incubated at 37 °C and examined after 24 h of incubation. MIC is defined as the lowest drug concentration able to inhibit the visible growth in comparison to the untreated control. The turbidity of the 96-well plate was also measured using a spectrophotometer (530 nm) (Multiskan EX, Thermo Scientific). *C. albicans* ATCC 10231 exhibited sensitivity to BFZ and CTZ showing MIC values of 2 and 0.0625 μg/mL respectively.

2.2.8. Preliminary anticandidal assay in agar plates

All the formulated IVRs (blank, 10% BFZ, and 10% CTZ) were preventively sterilized by UV radiation underflow safety cabinet for 1 h (30 min for each side) and then stored in sterile Petri dishes. The anticandidal assay was performed as previously reported [19]. Briefly, several colonies of *C. albicans* ATCC 10231 were inoculated into TSB (15 mL) and incubated at 37 °C for 24 h. The suspension was then quantified by spectrophotometer as described above and 500 μL of this culture was added to 25 mL of sterile SDA maintained at 50 °C and gently homogenised. At this point, 15 mL were rapidly poured into a Petri dish and allowed to solidify for several minutes; the formulated IVR was placed in the centre of the solidified layer and the remaining 10 mL of inoculated SDA were poured to englobe the medical device. This procedure was carried out for each formulated IVR in duplicate. The plates were incubated at 37 °C for 24 h, afterwards the presence of a well-defined zone of growth inhibition visible around each IVR, index of anticandidal activity, was observed and measured.

2.2.9. Time-kill assay

In this study, a VFS was used to simulate the typical vaginal environment of *Candida* infection. VFS was prepared as reported above and sterilized by filtration (0.22 μm) and maintained at 4 °C before use.

The day before the experiments, a series of sterile tubes with 20 mL of VFS were prepared and organized as follow: one tube with 10% CTZ IVR, one tube with 10% BFZ IVR, an done with blank IVR (control). The test organism was incubated in 15 mL of TSB at 37 °C for 24 h and, at the end of the incubation period, the suspension was centrifuged at 3500 rpm for 10 min, the pellet was resuspended in the same volume of VFS up to a turbidity of ca 10^6 CFU/mL. At this point, 1 mL of the inoculum was added to the different sterile tubes incubated at 37 °C with gentle shaking (100 rpm). At established time points (up to seven days: baseline, 24, 48, 72, 96, 120, 144, and 168 h), 100 μL aliquots were aseptically removed from each series, diluted in sterile physiological saline solution, and spread in triplicate (10 μL) onto SDA plates. After 24 h of incubation at 37 °C, the plates were observed for CFU/mL enumeration. All the experiments were performed in triplicate using independent cultures.

2.3. Statistical analysis

The student's t-test, paired with two tailed was employed to evaluate weather if the differences between the devices loaded with the two drugs were statistically significant ($p < 0.05$). All experiments were conducted at least in triplicate. Results were expressed as mean ± standard deviation.

3. Results and discussion

3.1. Fabrication and characterization of 3D printed IVRs

3D printed IVRs with 10% BFZ and 10% CTZ were produced by HME coupled with FDM technique. The design was chosen to comply with the already commercialized rings, the sizes of which are 54 mm of OD and 4 mm of CSD. Filaments and 3D printed rings were observed with a microscope to ensure the absence of aggregates as shown in Fig. 1. The blank and loaded filaments and IVRs presented a smooth and uniform surface. In particular, the blank IVRs were clear and transparent, while the drug loaded IVRs showed, respectively, intense white colour for the BFZ IVR, and a white to pale yellow for the CTZ IVR, due to the presence of the drugs, as already noticed during the HME process.

Immediately after printing, the rings were measured for their OD and weighted. The resulting measurements are reported in Table 2. All the

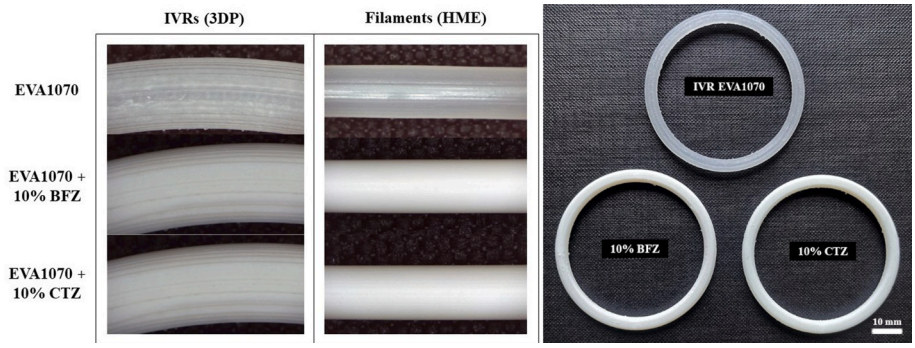

Fig. 1. Starting filaments and final IVRs observed with the stereo microscope.3D printed IVRs.

Table 2
Average dimensional and mass analysis of produced IVRs.

Sample	Weight (g)	OD (mm)	CSD (mm)
EVA	1.832 ± 0.005	53.66 ± 0.017	4.02 ± 0.005
EVA+ 10% BFZ	1.861 ± 0.009	53.12 ± 0.042	4.02 ± 0.008
EVA+ 10% CTZ	1.873 ± 0.003	53.12 ± 0.023	4.03 ± 0.008

manufactured devices were considered dimensionally accurate as they were within the specific acceptance criteria. Moreover, the reproducibility of the printing process was demonstrated.

3.2. Drug distribution evaluation

ATR-FTIR was performed to investigate the chemical composition of the printed IVRs. The resulting spectra are illustrated in Fig. 2. The spectra of the printed devices (EVA + 10% BFZ and EVA + 10% CTZ) presented the typical peaks of the polymer and the respective drug, suggesting that the physiochemical characteristics of the materials were maintained. Specifically, the characteristic peaks of EVA are at 1243 cm^{-1} (caused by the vibration of C–H), at 1740 cm^{-1} (due to the stretching vibration of C–O), at 2980 cm^{-1} (absorbance associated with –OH group vibrations), and bands at 1117 and 710 cm^{-1} (that reflects the vibrations of C–O and O–C–O groups, respectively), [31]. Regarding the APIs, numerous absorption bands in the fingerprint region can be observed. Given the chemical similarities, the FTIR spectra overlap. The most intense peaks are attributable to the imidazole ring (1000–650 cm^{-1} and 1680–1640 cm^{-1}) and the benzene rings (1600–1585 cm^{-1}). Specifically, the aromatic cycles stretch at 1570 cm^{-1}, 1487 cm^{-1}, the CH stretches in the 900-700 cm^{-1} domain, and 1206 $cm^{-1}$the CN stretching. In addition, CTZ shows the chlorobenzene stretch at around 1040 cm^{-1} [32,33].

Moreover, FTIR was employed to assess whether the APIs were uniformly incorporated into the final formulation, by comparing the peaks of random sections of the same sample. For this purpose, the EVA absorption at 2980 cm^{-1} was used as reference to normalize and compare the samples. As shown in Fig. 3, no significant differences in the intensities of the peaks were observed, confirming that the APIs were homogeneously distributed among the devices.

In addition, different pieces from the same device were cut, weighted, and then placed in ethanol under gentle stirring for 48 h. The quantification of the amount of drug released from each sample (data not shown) further confirmed the homogeneous distribution of the APIs.

3.3. Thermal behaviour

Since the production of the IVRs required two thermal processes, the stability of the drugs in the final formulations was evaluated using TGA (Fig. 4). In Table 3, the temperatures related to the onset degradation (T_{onset}) and the maximum rate of degradation (T_d) are reported, being evaluated through DTG (Fig. 4C–D). For the Eva, the two characteristic steps of degradation were observed: the first T_{onset} approximately at 320.61 °C, with a weight loss of just 1.55%, resulting from the loss of acetic acid; and the second step at 412.69 °C, with an additional weight loss of 10.16% and a T_d at 483.69 °C, attributable to the fragmentation of the polymer backbones [34]. TGA measurements of BFZ are shown in Fig. 4A, C: at the printing temperature (200 °C), BFZ proved to be thermally stable, starting to slightly degrade at 223.80 °C with a weight loss of 1.85%, and the T_d at 329.42 °C. The combination of the polymer and the drug leads to higher stability: the first T_{onset} of the final formulation falls at 250.89 °C, with a weight loss of 5.15%, while the second step of the degradation is at 408.1 °C, with a weight loss of 18.52% from the first T_{onset}; the T_d is recorded at 474.39 °C. Regarding CTZ, the first degradation occurs at 155 °C, being characterized by a weight loss of about 1%, which becomes more consistent at 218.65 °C, with a T_d weight loss of 4.67% and the T_d at 302.97 °C. As shown in Fig. 4B, even in this case, the combination of EVA with CTZ improves drug stabilization. Indeed, the initial degradation temperature of the IVR is higher than the one of the pure drug: the first T_{onset} is at 238.41 °C, with a weight loss of 1.17%; and a second T_{onset} at 414.02 °C, with a

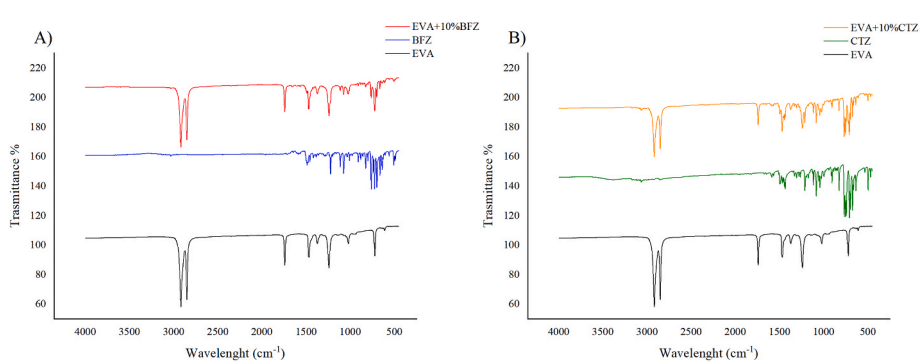

Fig. 2. A) FT-IR spectra of EVA, BFZ, and the final BFZ-loaded IVR. **B)** FT-IR spectra of EVA, CTZ, and the final CTZ-loaded IVR.

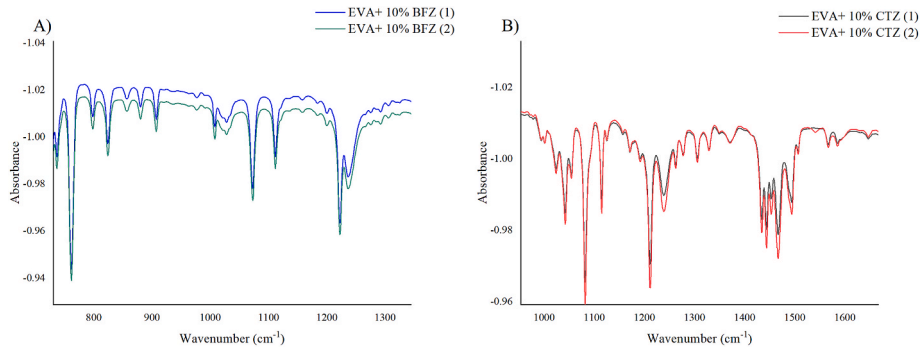

Fig. 3. Homogeneous distribution of the sample containing **A)** BFZ; **B)** CTZ evaluated by ATR-FTIR.

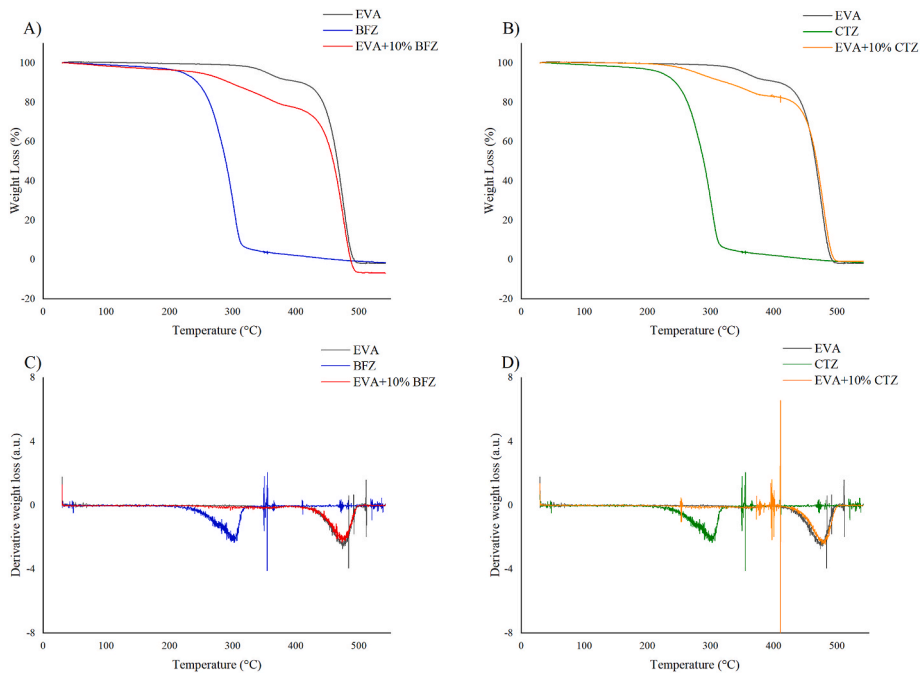

Fig. 4. A) TGA of EVA, BFZ, and EVA+10% BFZ; **B)** TGA of EVA, CTZ, and EVA+10% CTZ; **C)** DTG of EVA, BFZ, and EVA+10% BFZ; **D)** DTG of EVA, CTZ, and EVA+10% CTZ.

Table 3
Melting temperatures, crystallization degree, onset temperatures, and maximum rate of degradation of the samples.

Sample	*Tonset (°C)*	Td (°C)	Tm (°C)	χ (%)
EVA1070	320.61	483.69	97	14.2
BFZ	223.80	329.42	148	#
EVA+ 10% BFZ	250.89	474.39	97	14.4
CTZ	218.65	302.97	145	#
EVA + 10% CTZ	238.41	480.63	97	14.3

weight loss of 16.51% from the first step and the T_d at 480.63 °C. Overall, TGA measurements confirmed that BFZ and CTZ remained stable at the respective processing temperatures, in addition, results suggest that the polymer displays a protective effect toward the thermal degradation of both drugs [35]. Furthermore, TGA was employed to quantify the effective drug loaded into the devices. From the weight loss, it was calculated that for both IVRs, 9% of the respective drug was efficiently incorporated.

To investigate the effect of the API on the thermal behaviour of EVA, DSC analysis in the 30–200 °C range was carried out. In Fig. 5 the DSC thermograms of the printed samples (freshly prepared and after 4 weeks storage) and the starting materials, are shown. The melting peaks of EVA appear at about 97 °C; while the melting peaks of the BFZ and CTZ fall at 148 °C and 145 °C, respectively. EVA +10% BFZ thermograms reveal two endothermic events, one related to the polymer and the second one attributable to BFZ, suggesting that the drug preserves its crystalline structure within the matrix (Fig. 5A). On the other hand, in the EVA +10% CTZ formulation, the characteristic endothermic peak of CTZ disappears (Fig. 5B) and this could be attributed to the dissolution of the drug in the polymer or to the formation of an amorphous solid dispersion of the drug in the EVA matrix. For both devices, the analysis was also repeated after 4 weeks storage, providing information about the physical stability of the drug. The resulting thermograms did not show any significant difference compared to the freshly prepared devices, suggesting that the systems remained stable. Overall, the presence of the API did not affect the crystallinity (*χ (%)*) of EVA.

3.4. *In vitro drug release studies*

Despite the increase interest towards the application of IVRs as alternative delivery forms, at present there are no clear regulatory guidelines. However, some compendial and non-compendial methods have been proposed for QC and to predict the release performance [36].

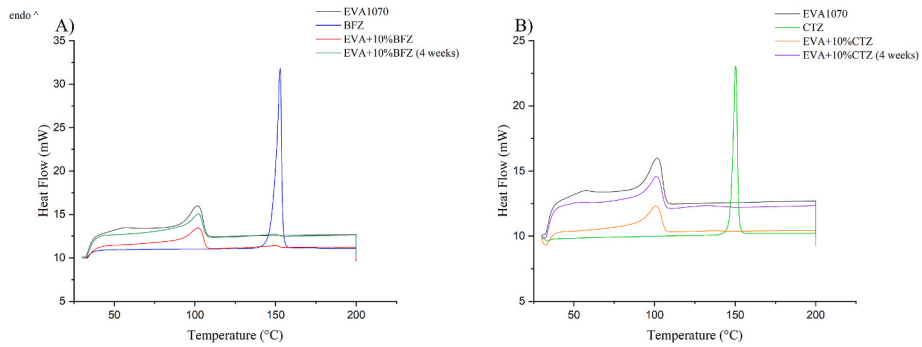

Fig. 5. DSC analysis of **A)** EVA +10% BFZ ring; **B)** EVA +10% CTZ ring.

Herein we evaluated the drug release of the IVRs in two different media: a mixture of water/ethanol was chosen for QC purpose; while the VFS at pH 4.2 was employed as biorelevant medium to predict the *in vivo* release [37,38]. Previous studies reported that the release profile from the EVA matrix is affected by several factors, including the crystallinity of the drug and the polymer, the drug loading, and the extrusion temperature. In addition, the release is influenced by the solubility of the drug in the dissolution medium [25], for this reason 1% of SLS was added to the VFS.

Fig. 6A–C shows the cumulative release profiles of the 3D printed drug loaded IVRs; while Fig. 6B–D reports the respective daily release. Both BFZ and CTZ loaded devices showed, a burst release for the first 24 h, being in accordance with previously reported studies, where EVA was employed as polymer matrix [22]. However, the release of the CTZ-IVR was faster than BFZ-IVR, this can be attributed to the fact that BFZ was in the crystalline form, as shown from the DSC thermograms, resulting in a slower release rate. In the water/ethanol media, higher percentages were detected for the CTZ-IVR. Given the low standard deviation values, this approached confirmed the uniformity between different batches. In the VFS, the release profiles of the drug were different, indeed CTZ-IVR has shown a sustained release of the drug during seven days, unlike BFZ-IVR demonstrated a more prolonged release, suggesting the possibility to customize the treatment according to the patient's need. For both formulations, the amount of drug released was higher than the MIC values measured for C albicans (2 μg/mL for BFZ-IVR and 0.0625 μg/mL for CTZ-IVR), suggesting a potential efficacy.

3.5. Mechanical properties

IVRs require specific mechanical characteristics, indeed they should be flexible to be comfortable, easily inserted and removed and to avoid mucosal damaging; but also robust to avoid undesired expulsion. Thus, testing the mechanical properties represents a key aspect. The flexural characteristics of the devices were evaluated by recording the maximum force necessary to compress the IVRs of 5 mm (Fig. 7). For the drug loaded IVRs, a higher force was required, suggesting that the presence of the drug exerted a reinforcing effect on the polymer, indeed, the IVRs were slightly stiffer. The formulation containing CTZ required the

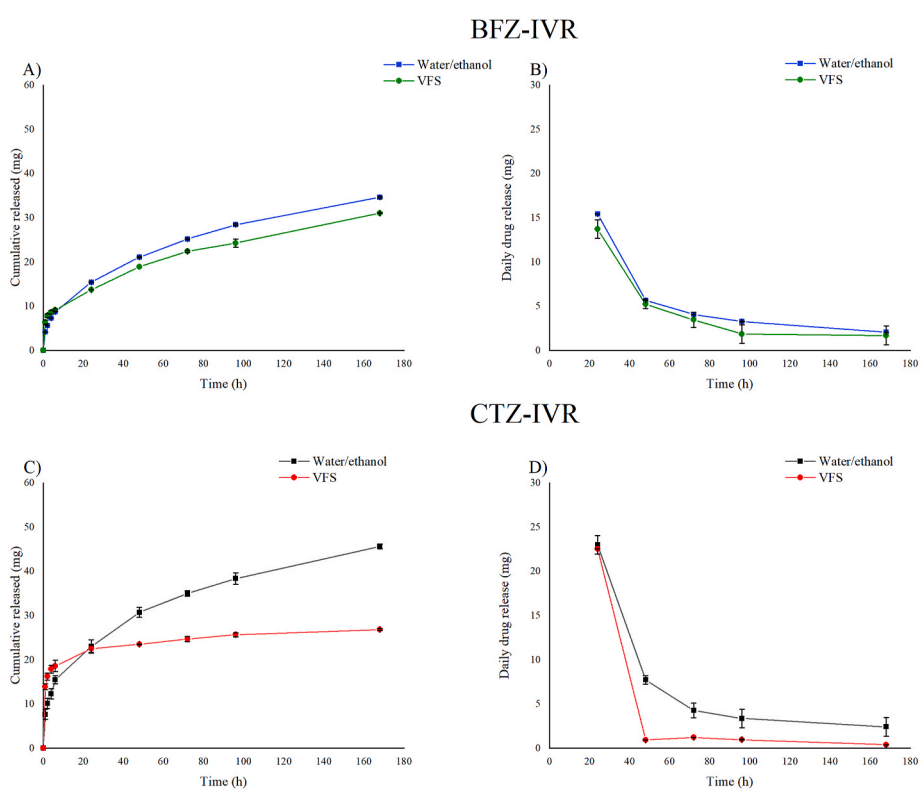

Fig. 6. Drug release from 3D printed 10% BFZ-IVR and CTZ-IVR. **A)** Cumulative BFZ release; **B)** Daily BFZ and release; **C)** Cumulative CTZ release; **D)** Daily CTZ release.

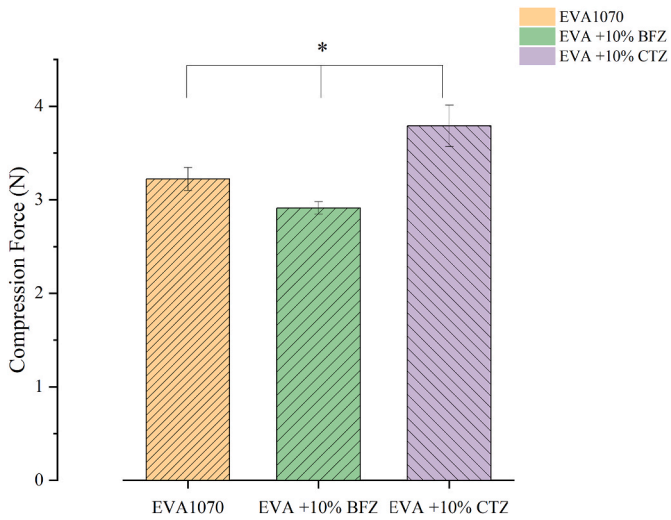

Fig. 7. Mechanical properties of the 3DP IVRs.

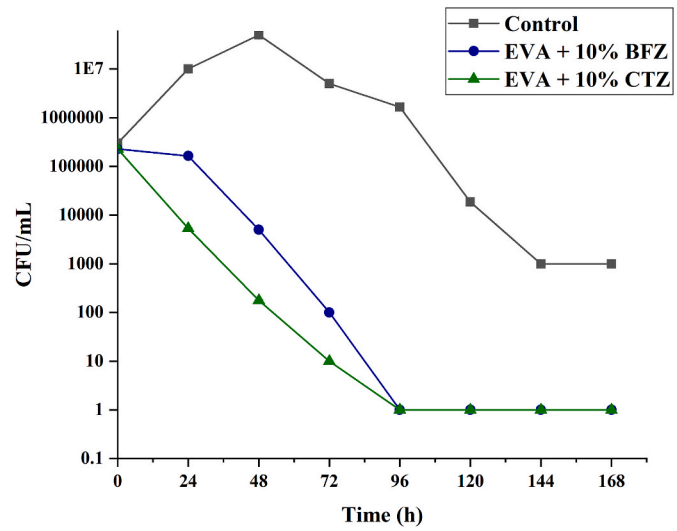

Fig. 9. Time-kill assay.

highest force to be compressed (3.8 N). Overall, the maximum forces recorded were lower than 4 N, complying with those of the commercially available products that can require forces up to 9 N [39,40].

3.6. Preliminary anticandidal assay in agar plates

The results related to the anti-*candida* activity of IVRs (10% BFZ and CTZ), and relative control (Blank IVR) are presented in Fig. 8. As expected, the control EVA-IVR without an antifungal agent showed no growth inhibition, while the presence of the drug-loaded IVRs resulted in a different inhibition of *C. albicans* ATCC 10231 growth. In the plate with 10% BFZ-IVR, the area of growth inhibition after 24 h was about 1.5 cm (considering the IVR itself). Instead, in the plate with 10% CTZ-IVR, the area of growth inhibition after 24 h was more remarkable than BFZ, and the growth of *C. albicans* ATCC 10231 was limited to the edge of the plate, away from the IVR, indicating the effectiveness of this type of formulation against the examined microorganism. This test confirmed that CTZ had a better release in 24 h than BFZ, as detected with the release test (in which we observed that the concentration released in the VFS, after one day, is about 14 mg for BFZ-IVR and about 23 mg for CTZ-IVR).

3.7. Time-kill assay

Time-kill experiments (Fig. 9) were performed to confirm the antifungal activity of the different IVRs (plain IVR made with EVA as control and drug loaded IVRs with 10% CTZ, and 10% BFZ) observed in the agar assay. As shown, after 24 h of incubation, the viability of *C. albicans* ATTC 10231 decreased to 5×10^3 CFU/mL in the presence of 10% CTZ IVR and to 1.6×10^5 CFU/mL in the presence of 10% BFZ-IVR, while in the control with plain EVA-IVR, the viability increased up to 1×10^7 CFU/mL. In the following time points (48 and 72 h) a more drastic decrease of the pathogen viability was observed in the presence of 10% CTZ-IVR with values ranging from 1.7×10^2 to 10 CFU/mL, reaching the complete growth inhibition (no detectable CFU/mL) after 96 h of incubation. With the 10% BFZ-IVR, the decrease of viability was slighter compared to that observed with 10% CTZ-IVR, with CFU/mL values ranging from 5×10^3 to 1×10^2 CFU/mL after 48 and 72 h of incubation respectively, reaching no detectable CFU/mL at 96 h. In the control, the growth of *C. albicans* ATCC 10231 continued with increasing CFU/mL values up to 48 h (5×10^7 CFU/mL) and then slightly decreased up to 1.2×10^6 CFU/mL after 96 h of incubation. In the final time points (up to 168 h), no CFU/mL were detectable in the presence of the two drug-loaded IVRs, while in the control in which the plain EVA-IVR was present, the viability of *Candida* decreased up to 1×10^3 CFU/mL. These results are aligned again with the faster release of CTZ compared to BFZ revealed in the drug release studies.

4. Conclusions

In this work, we successfully applied FDM 3DP technology to manufacture drug loaded matrix-type IVRs using EVA copolymer loaded with BFZ or CTZ as innovative antifungal medical devices. The employment of EVA as a matrix polymer allows to control the drug release profile giving the possibility to apply IVRs as a new treatment strategy against fungal infections. Thus, the printed IVRs can be considered as an alternative to oral antifungals for immediate treatment and/or for maintenance therapy in case of recurrences. In addition, since the common treatment for fungal infections consists of multiple applications of conventional dosage forms, the utilization of an intravaginal device (such as the BFZ- or the CTZ-loaded rings) could improve patient

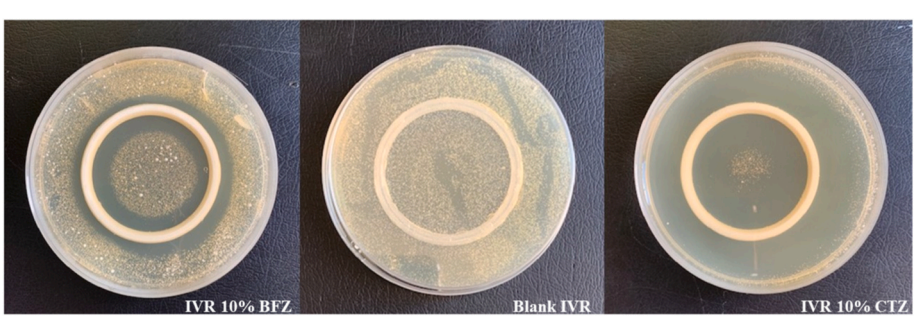

Fig. 8. Preliminary antifungal activity of prepared IVRs, assessed by a modified agar-diffusion method.

compliance by decreasing the number of applications to one, switching from a daily to a weekly therapy. The advantages of 3DP as manufacturing technique are well established, however, despite the increase interest in proving its feasibility to produce drug delivery forms, at present, there are only few studies reporting its applicability for intravaginal devices. The present work represents a step forward in the development of antifungal intravaginal medical devices that can be produced in small batches by 3D printing for personalized therapy or clinical studies.

CRediT authorship

Sofia Moroni: Methodology, Investigation, Formal analysis, Data curation, Writing - original draft., Annalisa Aluigi, Francesca Bischi, and Raffaella Campana: Methodology, Data curation, Writing - review & editing., Mattia Tiboni: Conceptualization, Supervision, Methodology, Formal analysis, Data curation, Writing - review & editing, Luca Casettari: Conceptualization, Resources, Funding acquisition, Project administration, Supervision, Writing - review & editing.

Funding

Sofia Moroni acknowledge Marche Region for the PhD scholarship (Innovative doctoral programme POR Marche FSE 2014/2020 D.R. 354/2020).

This project received support from the European Union – Next Generation EU - PNRR MUR project ECS_00000041-VITALITY.

Declaration of competing interest

The authors declare no conflict of interest.

Data availability

Data will be made available on request.

Acknowledgements

We would like to express our sincere gratitude to Celanese for their contribution to this research and for providing Celanese EVA (ethylene vinyl acetate) used in this study as well as the support to article review. Moreover, we acknowledge ITIS E. Mattei (Urbino, PU, Italy) for the utilization of FT-IR instrument.

References

[1] J.D. Sobel, Vulvovaginal candidosis, Lancet 369 (2007) 1961–1971, https://doi.org/10.1016/S0140-6736(07)60917-9.
[2] B. Gonçalves, C. Ferreira, C.T. Alves, M. Henriques, J. Azeredo, S. Silva, Vulvovaginal candidiasis: epidemiology, microbiology and risk factors, Crit. Rev. Microbiol. 42 (2016) 905–927, https://doi.org/10.3109/1040841X.2015.1091805.
[3] M. Gulati, C.J. Nobile, Candida albicans biofilms: development, regulation, and molecular mechanisms, Microb. Infect. 18 (2016) 310–321, https://doi.org/10.1016/j.micinf.2016.01.002.
[4] T.M. Dall, S.E. Mann, Y. Zhang, W.W. Quick, R.F. Seifert, J. Martin, E.A. Huang, S. Zhang, Distinguishing the economic costs associated with type 1 and type 2 diabetes, Popul. Health Manag. 12 (2009) 103–110, https://doi.org/10.1089/POP.2009.12203.
[5] A. Spinillo, E. Capuzzo, S. Nicola, F. Baltaro, A. Ferrari, A. Monaco, The impact of oral contraception on vulvovaginal candidiasis, Contraception 51 (1995) 293–297, https://doi.org/10.1016/0010-7824(95)00079-P.
[6] J. Yano, J.D. Sobel, P. Nyirjesy, R. Sobel, V.L. Williams, Q. Yu, M.C. Noverr, P. L. Fidel, Current patient perspectives of vulvovaginal candidiasis: incidence, symptoms, management and post-treatment outcomes, BMC Wom. Health 19 (2019) 1–9, https://doi.org/10.1186/s12905-019-0748-8.
[7] H.S. Johal, T. Garg, G. Rath, A.K. Goyal, Advanced topical drug delivery system for the management of vaginal candidiasis, Drug Deliv. 23 (2016) 550–563, https://doi.org/10.3109/10717544.2014.928760.
[8] A. Farr, I. Effendy, B. Frey Tirri, H. Hof, P. Mayser, L. Petricevic, M. Ruhnke, M. Schaller, A.P.A. Schaefer, V. Sustr, B. Willinger, W. Mendling, Guideline: vulvovaginal candidosis (AWMF 015/072, level S2k), Mycoses 64 (2021) 583–602, https://doi.org/10.1111/myc.13248.
[9] S. Aballéa, F. Guelfucci, J. Wagner, A. Khemiri, J.P. Dietz, J. Sobel, M. Toumi, Subjective health status and health-related quality of life among women with Recurrent Vulvovaginal Candidosis (RVVC) in Europe and the USA, Health Qual. Life Outcome 11 (2013) 1–13, https://doi.org/10.1186/1477-7525-11-169.
[10] D.W. Denning, M. Kneale, J.D. Sobel, R. Rautemaa-Richardson, Global burden of recurrent vulvovaginal candidiasis: a systematic review, Lancet Infect. Dis. 18 (2018) e339–e347, https://doi.org/10.1016/S1473-3099(18)30103-8.
[11] J. Conte, A.L. Parize, T. Caon, Advanced solid formulations for vulvovaginal candidiasis, Pharm. Res. (N. Y.) (2022) 593–610, https://doi.org/10.1007/s11095-022-03441-5.
[12] L. Carson, R. Merkatz, E. Martinelli, P. Boyd, B. Variano, T. Sallent, R.K. Malcolm, The vaginal microbiota, bacterial biofilms and polymeric drug-releasing vaginal rings, Pharmaceutics 13 (2021) 1–28, https://doi.org/10.3390/pharmaceutics13050751.
[13] P. Boyd, I. Major, W. Wang, C. McConville, Development of disulfiram-loaded vaginal rings for the localised treatment of cervical cancer, Eur. J. Pharm. Biopharm. 88 (2014) 945–953, https://doi.org/10.1016/j.ejpb.2014.08.002.
[14] J.B. Griffin, K. Ridgeway, E. Montgomery, K. Torjesen, R. Clark, J. Peterson, R. Baggaley, A. van der Straten, Vaginal ring acceptability and related preferences among women in low- and middle-income countries: a systematic review and narrative synthesis, PLoS One 14 (2019) 1–22, https://doi.org/10.1371/journal.pone.0224898.
[15] J. Kerns, P. Darney, Vaginal ring contraception, Contraception 83 (2011) 107–115, https://doi.org/10.1016/j.contraception.2010.07.008.
[16] F. Donath, L. Hoffmann, M. Todorova-Sanjari, R.S. Wedemeyer, A. Warnke, K. Nickisch, Intravaginal tolterodine formulation intended for overactive bladder treatment—results of a pharmacokinetic phase I pilot study in healthy, postmenopausal women, Clin. Pharmacol. Drug Dev. 11 (2022) 80–90, https://doi.org/10.1002/cpdd.968.
[17] I.C. Young, S.R. Benhabbour, Multipurpose prevention technologies: oral, parenteral, and vaginal dosage forms for prevention of hiv/stis and unplanned pregnancy, Polymers 13 (2021), https://doi.org/10.3390/polym13152450.
[18] Y. Wang, P. Boyd, A. Hunter, R.K. Malcolm, Intravaginal rings for continuous low-dose administration of cervical ripening agents, Int. J. Pharm. 549 (2018) 124–132, https://doi.org/10.1016/j.ijpharm.2018.07.053.
[19] M. Tiboni, R. Campana, E. Frangipani, L. Casettari, 3D printed clotrimazole intravaginal ring for the treatment of recurrent vaginal candidiasis, Int. J. Pharm. 596 (2021), 120290, https://doi.org/10.1016/j.ijpharm.2021.120290.
[20] C. Kaynak, Performance Comparison of the 3D-Printed and Injection-Molded PLA and its Elastomer Blend and Fiber Composites, 2019, https://doi.org/10.1177/0892705718772867.
[21] V.M. Vaz, L. Kumar, 3D printing as a promising tool in personalized medicine, AAPS PharmSciTech 22 (2021), https://doi.org/10.1208/s12249-020-01905-8.
[22] V. de Carvalho Rodrigues, I.Z. Guterres, B.P. Savi, I.T. Silva, G. Fongaro, G. V. Salmoria, 3D-Printed EVA devices for antiviral delivery and herpes virus control in genital infection, Viruses 14, https://doi.org/10.3390/v14112501, 2022.
[23] Y. Chen, Y.L. Traore, L. Walker, S. Yang, E.A. Ho, Fused deposition modeling three-dimensional printing of flexible polyurethane intravaginal rings with controlled tunable release profiles for multiple active drugs, Drug Deliv. Transl. Res. 12 (2022) 906–924, https://doi.org/10.1007/s13346-022-01133-6.
[24] R. Januszewicz, S.J. Mecham, K.R. Olson, S.R. Benhabbour, Design and characterization of a novel series of geometrically complex intravaginal rings with digital light synthesis, Adv. Mater. Technol. 5 (2020) 1–16, https://doi.org/10.1002/admt.202000261.
[25] N. Genina, J. Holländer, H. Jukarainen, E. Mäkilä, J. Salonen, N. Sandler, Ethylene vinyl acetate (EVA) as a new drug carrier for 3D printed medical drug delivery devices, Eur. J. Pharmaceut. Sci. 90 (2016) 53–63, https://doi.org/10.1016/j.ejps.2015.11.005.
[26] A.M. Henderson, Ethylene-vinyl Acetate (EVA) Copolymers: a General Review, 1993.
[27] NuvaRing ® (etonogestrel/ethinyl Estradiol Vaginal Ring) | Official Site ([WWW Document], n.d).
[28] N. Dumpa, A. Butreddy, H. Wang, N. Komanduri, S. Bandari, M.A. Repka, 3D printing in personalized drug delivery : an overview of hot-melt extrusion-based fused deposition modeling, Int. J. Pharm. 600 (2021), 120501, https://doi.org/10.1016/j.ijpharm.2021.120501.
[29] L. Kasper, P. Miramón, N. Jablonowski, S. Wisgott, D. Wilson, S. Brunke, B. Hube, Antifungal activity of clotrimazole against Candida albicans depends on carbon sources, growth phase and morphology, J. Med. Microbiol. 64 (2015) 714–723, https://doi.org/10.1099/jmm.0.000082.
[30] A. Espinel-Ingroff, A. Fothergill, M. Ghannoum, E. Manavathu, L. Ostrosky-Zeichner, M.A. Pfaller, M.G. Rinaldi, W. Schell, T.J. Walsh, Quality control and reference guidelines for CLSI Broth microdilution method (M38-A document) for susceptibility testing of anidulafungin against molds, J. Clin. Microbiol. 45 (2007) 2180, https://doi.org/10.1128/JCM.00399-07.
[31] P. Agarwal, M.K. Nieuwoudt, S. Li, G. Procter, G.P. Andrews, D.S. Jones, D. Svirskis, Exploiting hydrogen bonding to enhance lidocaine loading and stability in a poly ethylene-co-vinyl acetate carrier matrix, Int. J. Pharm. 621 (2022), https://doi.org/10.1016/j.ijpharm.2022.121819.
[32] H. Kelemen, A. Csillag, G. Hancu, B. Székely-Szentmiklósi, I. Fülöp, E. Varga, L. Grama, G. Orgován, Characterization of inclusion complexes between bifonazole and different cyclodextrins in solid and solution state, Maced. J. Chem. Chem. Eng. 36 (2017) 81–91, https://doi.org/10.20450/mjcce.2017.1031.

[33] P. Tonglairoum, T. Ngawhirunpat, T. Rojanarata, S. Panomsuk, R. Kaomongkolgit, P. Opanasopit, Fabrication of mucoadhesive chitosan coated polyvinylpyrrolidone/cyclodextrin/clotrimazole sandwich patches for oral candidiasis, Carbohydr. Polym. 132 (2015) 173–179, https://doi.org/10.1016/j.carbpol.2015.06.032.

[34] G. Maurizii, S. Moroni, S. Khorshid, A. Aluigi, M. Tiboni, L. Casettari, 3D-printed EVA-based patches manufactured by direct powder extrusion for personalized transdermal therapies, Int. J. Pharm. 635 (2023), 122720, https://doi.org/10.1016/j.ijpharm.2023.122720.

[35] P. Garcia Ferreira, C. Guimarães de Souza Lima, L.L. Noronha, M.C. de Moraes, F. de C. da Silva, A. Lifsitch Viçosa, D. Omena Futuro, V. Francisco Ferreira, Development of a method for the quantification of clotrimazole and itraconazole and study of their stability in a new microemulsion for the treatment of sporotrichosis, Molecules 24 (2019), https://doi.org/10.3390/MOLECULES24122333.

[36] K. Tietz, S. Klein, In vitro methods for evaluating drug release of vaginal ring formulations—a critical review, Pharmaceutics 11 (2019), https://doi.org/10.3390/pharmaceutics11100538.

[37] P. Boyd, B. Variano, P. Spence, C.F. McCoy, D.J. Murphy, Y.H. Dallal Bashi, R. K. Malcolm, In vitro release testing methods for drug-releasing vaginal rings, J. Contr. Release (2019), https://doi.org/10.1016/j.jconrel.2019.10.015.

[38] C. McConville, J.M. Smith, C.F. McCoy, P. Srinivasan, J. Mitchell, A. Holder, R. A. Otten, S. Butera, G.F. Doncel, D.R. Friend, R.K. Malcolm, Lack of in vitro–in vivo correlation for a UC781-releasing vaginal ring in macaques, Drug Deliv. Transl. Res. 5 (2015) 27–37, https://doi.org/10.1007/s13346-015-0216-4.

[39] N.R. Welsh, R.K. Malcolm, B. Devlin, P. Boyd, Dapivirine-releasing vaginal rings produced by plastic freeforming additive manufacturing, Int. J. Pharm. 572 (2019), 118725, https://doi.org/10.1016/j.ijpharm.2019.118725.

[40] N. Promadej-Lanier, J.M. Smith, P. Srinivasan, C.F. McCoy, S. Butera, A. D. Woolfson, R.K. Malcolm, R.A. Otten, Development and evaluation of a vaginal ring device for sustained delivery of HIV microbicides to non-human primates, J. Med. Primatol. 38 (2009) 263–271, https://doi.org/10.1111/j.1600-0684.2009.00354.x.